Effect of deposition conditions on the physical properties of Sn_xS_y thin films prepared by the spray pyrolysis technique

M. R. Fadavieslam[1, 2, †], N. Shahtahmasebi[1], M. Rezaee-Roknabadi[1], and M. M. Bagheri-Mohagheghi[2]

[1]Nanotechnology Research Center, Department of Physics, Faculty of Basic Sciences, Ferdowsi University of Mashhad, Mashhad, Iran
[2]School of Physics, Damghan University, Damghan, Iran

Abstract: Tin sulfide thin films (Sn_xS_y) with an atomic ratio of $y/x = 0.5$ have been deposited on a glass substrate by spray pyrolysis. The effects of deposition parameters, such as spray solution rate (R), substrate temperature (T_s) and film thickness (t), on the structural, optical, thermo-electrical and photoconductivity related properties of the films have been studied. The precursor solution was prepared by dissolving tin chloride ($SnCl_4$, $5H_2O$) and thiourea in propanol, and Sn_xS_y thin film was prepared with a mole ratio of $y/x = 0.5$. The prepared films were characterized by X-ray diffraction (XRD), scanning electron microscopy (SEM) and UV-vis spectroscopy. It is indicated that the XRD patterns of Sn_xS_y films have amorphous and polycrystalline structures and the size of the grains has been changed from 7 to 16 nm. The optical gap of Sn_xS_y thin films is determined to be about 2.41 to 3.08 eV by a plot of the variation of $(\alpha h\nu)^2$ versus $h\nu$ related to the change of deposition conditions. The thermoelectric and photo-conductivity measurement results for the films show that these properties are depend considerably on the deposition parameters.

Key words: thin film; tin sulfide; spray pyrolysis; photoconductivity
DOI: 10.1088/1674-4926/32/11/113002 **EEACC:** 2520

1. Introduction

SnS is a very important optical semiconductor, which can exhibit both p-and n-type conduction, depending on the mole concentration of tin and sulfur. SnS thin film has an energy band gap of about 1.3 eV between Si and GaAs. Like SnS, SnS_2 is also a semiconductor, with a larger band gap of 2.2–2.6 eV. The electronic nature and excellent structural properties of SnS_2 make it a possible candidate for use as the aperture in window-absorber solar cells, quantum well structures and the substrate for deposition of organic layers[1−3]. The constituent element of tin sulfide such as 'Sn' and 'S' are abundant in nature, less toric and available at low cost.

Sn_xS_y thin films have been deposited by variety of physical and chemical techniques, such as chemical vapor deposition (CVD), electro deposition, chemical bath deposition, spray pyrolysis, electron beam-induced deposition and vacuum evaporation[4]. However, the spray pyrolysis technique is a relatively simple, atmospheric-pressure deposition method and convenient for the large area deposition of IV–VI semiconductor compounds.

The systematic investigation of the effect of deposition parameters on the photoconductivity properties of Sn_xS_y films in photovoltaic applications is as important as it is in opto-electronic devices. The electronic and optical properties of tin sulfide could be controlled by deposition parameters. In this paper, we investigate the effects of deposition parameters such as spray solution rate (R), substrate temperature (T_s) and film thickness (t) on the physical properties of the chemically sprayed Sn_xS_y thin films with $y/x = 0.5$ for photovoltaic applications.

2. Experimental procedure

2.1. Deposition of Sn_xS_y films by the spray pyrolysis technique

The Sn_xS_y thin films were deposited on glass substrates using a typical spray pyrolysis coating system as seen in Fig. 1[5]. The precursor solution was prepared by dissolving 0.0427 M of tin chloride ($SnCl_4$, $5H_2O$) and 0.0213 M of thiourea in 100 ml propanol, and the Sn_xS_y thin film was prepared with a mole ratio of $y/x = 0.5$. The Sn_xS_y thin films were deposited under similar conditions: nozzle-to-substrate

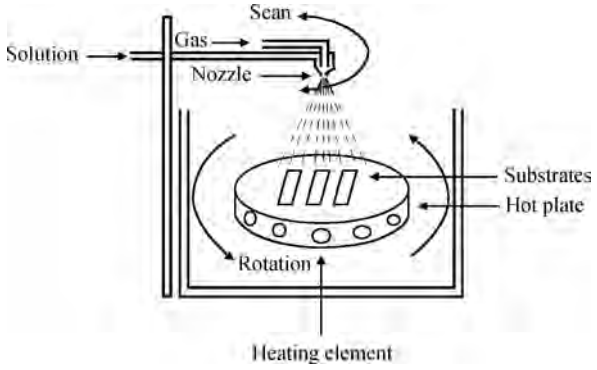

Fig. 1. Basic set-up for spray deposition.

† Corresponding author. Email: fadavieslam@yahoo.com
Received 18 March 2011, revised manuscript received 5 July 2011

Table 1. Spray deposition parameters for preparation of Sn_xS_y films.

	(a) Effect of spray rate	(b) Effect of substrate temperature	(c) Effect of volume of spray solution
Volume of spray solution (mL)	100	100	25, 50, 100, 150
Spray rate (mL/min)	2, 5, 10, 15	10	10
Substrate temperature (℃)	420	320, 370, 420, 470	420
Carrier-gas pressure (atm)	2.5	2.5	2.5
Nozzle–to-substrate distance (cm)	35	35	35
Hot plate rotation speed (rpm)	60	60	60
Spray nozzle diameter (mm)	0.2	0.2	0.2

Table 2. X-ray diffraction results for sprayed Sn_xS_y thin films for (001) orientation.

Sn_xS_y: $y/x = 0.5$	2θ (°)	FWHM (°)	Mean grain size (nm)	Lattice distance (Å) Observed	Standard	Identification with (hkl) value
(a) Effect of spray rate (Volume = 100 cc, T_s = 420 ℃)						
2 mL/min	—	—	—	—	—	—
5 mL/min	—	—	—	—	—	—
10 mL/min	14.76	0.8	10.2	5.88	5.81	Hexagonal-SnS_2
15 mL/min	14.92	0.77	10.6	5.92	5.81	Hexagonal-SnS_2
(b) Effect of substrate temperature (Rate = 10 mL/min, Volume = 100 cc)						
320 ℃	14.92	0.9	7.3	5.93	5.81	Hexagonal-SnS_2
370 ℃	14.72	1.11	9.1	6.01	5.81	Hexagonal-SnS_2
420 ℃	14.76	0.8	10.2	5.88	5.81	Hexagonal-SnS_2
470 ℃	—	—	—	—	—	—
(c) Effect of volume of spray solution (T_s = 420 ℃, Rate = 10 mL/min)						
25 cc	—	—	—	—	—	—
50 cc	15	0.7	11.7	5.9	5.81	Hexagonal-SnS_2
100 cc	14.76	0.8	10.2	5.88	5.81	Hexagonal-SnS_2
150 cc	14.96	0.48	16.9	5.92	5.81	Hexagonal-SnS_2

distance (d) = 35 cm, carrier gas pressure (P_{air}) = 2.5 atm and hot plate rotation (r) = 60 rpm. To find the optimal parameters for the deposition of films (spray solution rate, substrate temperature and film thickness), three sets of experiments were carried out. In the first stage, in order to study of the effect of the spray solution rate on the physical properties of the thin films, the spray deposition was carried out at different rates with a choice of 2, 5, 10 and 15 mL/min. In the second stage, in order to study the substrate temperature effect, the substrate temperature was changed in the 320–470 ℃ region, with a step of 50 ℃. In the third stage, the thin films were deposited with different volumes of spray solution as 25, 50, 100, and 150 cc. Before preparation of the films, glass substrates were cleaned and placed on a hot plate, and the Sn_xS_y films were deposited on rotating hot substrates with the conditions mentioned in Table 1. To prevent a rapid reduction in the hot plate temperature, spraying was done in short time intervals. In each stage, only one parameter was changed and the other deposition parameters were approximately fixed.

2.2. Structural and optical characterization of films

For structural study of the films, X-ray diffraction (XRD) patterns of the Sn_xS_y films were recorded by a D8 Advance Bruker system using CuKα (λ = 0.154056 nm) radiation with 2θ in the range 10°–70°. The average crystalline size was calculated using Scherrer's formula[6]:

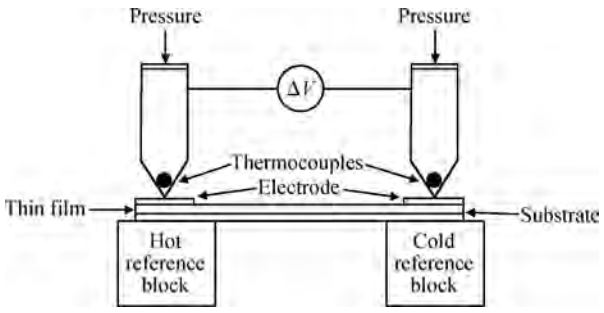

Fig. 2. Basic set-up for thermoelectric power measurement.

$$D = \frac{k\lambda}{\delta \cos\theta}, \tag{1}$$

where D is the average crystalline (grain) size, k is a constant (∼1), λ is the X-ray wavelength, δ is the full width at half maximum (FWHM) of the XRD peaks and θ is the Bragg angle.

The crystalline structure of the films was compared with the standard JCPDS data file No.83-1705 corresponding to the phase SnS_2. The XRD parameters and mean grain size of the films with various conditions have been summarized in Table 2.

The surface morphology of the films was studied by scanning electron microscopy (SEM) using an LEO 1450 VP system.

The optical absorption and transparency of the films were

Table 3. Optical, electrical and thermo-electrical measurement results of Sn_xS_y films for various spray rates.

Rate of spray R (mL/min)	Thickness t (nm)	Color	Energy gap E_g (eV)	Resistivity ρ_d (Ω·cm)	Conductivity type	Seebeck coefficient (mV/K) $T = 350$ K	Photosensitivity S $\mid \Delta R/R \mid$
2	402	Light yellow	2.41	1.87	p	1.08	0.12
5	495	Light yellow	2.53	7.26	p	0.06	0.12
10	568	Brick red	2.73	2.34	p	4.6	0.1
15	612	Black brick red	2.96	2.98	p	1.28	0.13

Table 4. Optical, electrical and thermoelectrical measurement results of Sn_xS_y films for various substrate temperatures.

Substrate temperature T_s (℃)	Thickness t (nm)	Color	Energy gap E_g (eV)	Resistivity ρ_d (Ω·cm)	Conductivity type	Seebeck coefficient (mV/K) $T = 350$ K	Photosensitivity (S) $\mid \Delta R/R \mid$
320	550	Light yellow	3.05	7.63×10^3	-	-	-
370	563	Yellow	2.71	1.75×10^3	p	3.15	0.14
420	568	Brick red	2.73	2.34	p	4.6	0.1
470	600	Black brick red	2.55	2.27	n	−0.19	0.4

Table 5. Optical, electrical and thermoelectrical measurement results of Sn_xS_y films for various solution volumes.

Volume of solution (cc)	Thickness t (nm)	Color	Energy gap E_g (eV)	Resistivity ρ_d (Ω·cm)	Conductivity type	Seebeck coefficient (mV/K) $T = 350$ K	Photosensitivity (S) $\mid \Delta R/R \mid$
25	243	Light yellow	3.08	3.62×10	p	0.43	0.04
50	461	Yellow	2.98	3.13	p	4.46	0.09
100	568	Brick red	2.73	2.34	p	4.6	0.1
150	623	Black brick red	2.55	1.66	n	−0.25	0.13

measured in the wavelength range of 300–1100 nm using an Agilent 8453 UV-vis single beam spectrophotometer at room temperature. The thickness (t) of the films was determined using the Swanepole method[7]. The direct optical band gap (E_g) of the prepared Sn_xS_y films was obtained by optical absorption measurements and plotting $(\alpha h\nu)^2$ versus photon energy ($h\nu$) and using the following relation[8]:

$$(\alpha h\nu)^2 = A(h\nu - E_g) \tag{2}$$

where α is the absorption coefficient, and A and E_g are the constant and direct band gap of the material, respectively.

2.3. Photo-electrical and thermoelectrical measurements

To measure the photo-electrical force and the thermoelectric electro-motive force (e.m.f.) of the films, two ends of the samples were coated with aluminum by thermal evaporation in vacuum using an Edwards E-306A coating system. The electrical resistivity of the Sn_xS_y films on the non-conducting glass slide was determined by the DC two-probe method and electrical conductivity (dark and light) was obtained for all the samples.

The photosensitivity of the films was measured as $S = \frac{R_L - R_d}{R_d}$[9], where R_L and R_d are the electrical resistance under illumination (9000 Lux) and in the dark, respectively. All the samples were illuminated at a distance (d) = 35 cm from a normal light source (150 W) for 100 s before recording R_L. The electrical resistance of the thin films was measured by UNI-T multi-meters and the light intensity was measured by a TES-1339 light meter.

The thermoelectric e.m.f. of the Sn_xS_y films was measured by applying a temperature gradient between the two ends of the samples at a temperature range of 300–500 K[10]. An electric heater with an electrical power of 300 W for heating one side (hot-side) and an ice-water bath for cooling the other side (cold-side) were utilized. The schematic view of the apparatus is shown in Fig. 2.

The open-circuit thermo-voltage generated by the samples under the temperature gradient was measured using a digital micro-voltmeter. The temperature difference between the two ends of the sample causes transport of carriers from the hot side to cold end, thus creating an electric field and voltage between the two ends. The thermo-voltage generated is directly proportional to the temperature gradient applied to the two ends of the samples. From the sign of the potentiometer terminals connected to the two ends of sample, the sign of the charge carrier is obtained. In this measurement, the negative and positive terminals were connected to the hot and cold ends, respectively. Therefore, the films show n or p-type conductivity.

According to the Seebeck effect[11], thermoelectric power (TEP) is calculated by

$$\varepsilon = \alpha \Delta T, \tag{3}$$

where ε is e.m.f, α is the Seebeck coefficient and ΔT is the temperature difference of the edges of the sample. Indeed, the thermo-electromotive force ΔV is proportional to the temperature difference of the edges of the sample (ΔT). The Seebeck coefficients (α) were determined by calculating the slope of the thermoelectric e.m.f. versus the temperature difference between the hot and the cold ends of the samples.

The optical, electrical and thermo-electrical measurement

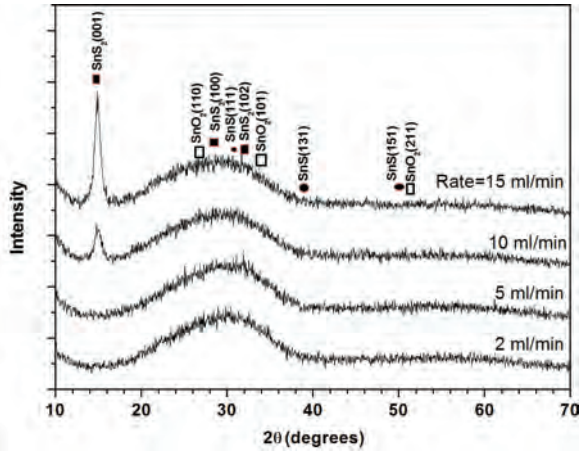

Fig. 3. X-ray diffraction patterns of Sn_xS_y thin films prepared by various solution rates.

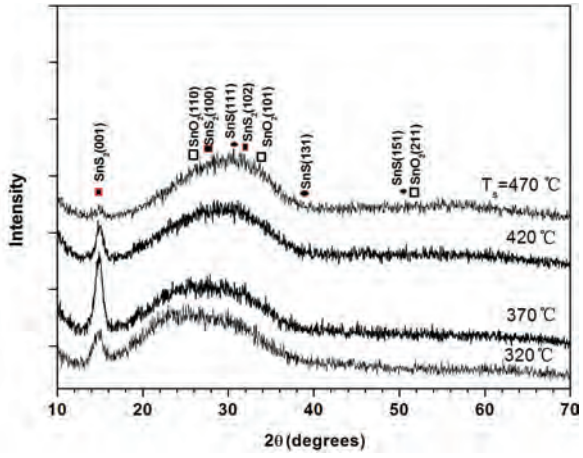

Fig. 4. X-ray diffraction patterns of Sn_xS_y thin films prepared by various substrate temperatures.

results of Sn_xS_y films for various deposition conditions have been summarized in Tables 3–5.

3. Results and discussion

3.1. Structural properties

3.1.1. Effect of spray rate (R)

Figure 3 shows the XRD patterns of the deposited Sn_xS_y films with different spray rates. The XRD patterns of thin films prepared with spray rates of 2 and 5 mL/min display an amorphous structure and thin films prepared by solution rates of 10 and 15 mL/min display a polycrystalline structure corresponding to SnS_2 and SnO_2 phases. The grain size in direction of the (001) hexagonal plane of SnS_2 film for different spray rates of 10 and 15 mL/min, are indicated to be 10.2 and 10.6 nm, respectively (see Table 2).

Furthermore, with increasing the solution spraying rate from 2 to 15 mL/min, the opacity of the films decrease so that, in 2 mL/min, films are slightly black and in 15 mL/min slightly clear.

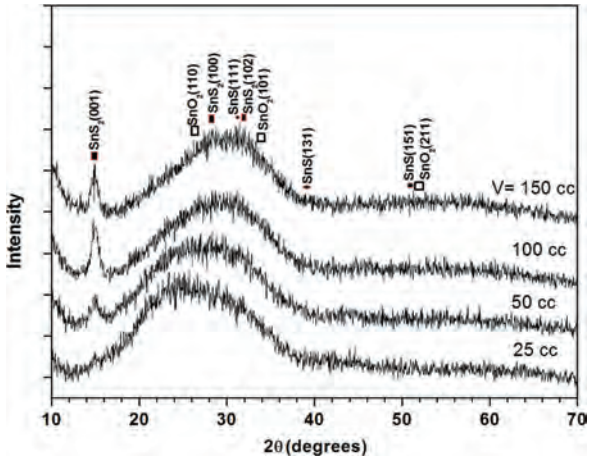

Fig. 5. X-ray diffraction patterns of thin films prepared by various spray solution volumes.

3.1.2. Effect of substrate temperature (T_s)

Figure 4 shows the XRD patterns of the deposited Sn_xS_y films with different substrate temperatures. Study of the XRD patterns of films prepared with various substrate temperatures indicates that $T_s = 370$ ℃ is the best substrate temperature for the highest structural order. Increasing the substrate temperature higher than 370 ℃ would lead to the scope of sulfur from the lattice and, finally, the formation of an amorphous structure. As can be seen, the temperature range of 320–370 ℃ corresponds to the highest domination of the SnS_2 phase[12]. When T_s increases to 420 ℃, the peak corresponding to SnS_2 disappears. The grain sizes in the direction of the (001) hexagonal plane of SnS_2 thin films calculated in $2\theta \approx 15°$ for substrate temperatures 320, 370 and 420 ℃ are 7.3, 9.1 and 10.2 nm, respectively (see Table 2). With an increase in the substrate temperature, the size of the grains is also increased[13].

The creation of the sulfur vacancy at higher temperatures is due to the high vapor pressure of sulfur, which increases rapidly with substrate temperature[8]. Moreover, by increasing the substrate temperature from 320 to 470 ℃, the color of the films become darker so that at $T_s = 320$ ℃, the color of films is light yellow but it is black brick red at 470 ℃, which shows that it depends on the perfect substitution of sulfur in the lattice.

3.1.3. Effect of volume of spray solution (V)

Figure 5 shows the XRD patterns of the deposited Sn_xS_y films with different spray solutions of 25 cc, 50 cc, 100 and 150 cc. The XRD pattern of the prepared films by a solution volume of 25 cc indicates an amorphous structure and the prepared films by solution volumes 50 cc, 100 cc, and 150 cc indicate a polycrystalline structure. Crystallinity seems to be improved as the film thickness increases with increasing the volume of spray solution from 25 cc to 150 cc[14]. The size of the grains in the (001) direction plane of SnS_2 thin films is calculated in $2\theta \approx 15°$ for solution volumes 50 cc, 100 cc and 150 cc is 11.7, 10.2 and 16.9 nm, respectively (See Table 2).

Also, with increasing the volume of spray solution from 25 cc to 150 cc, because of the increase of film thickness, the color of the films becomes darker.

The SEM images of films prepared at (a) $T_s = 370$ ℃ and

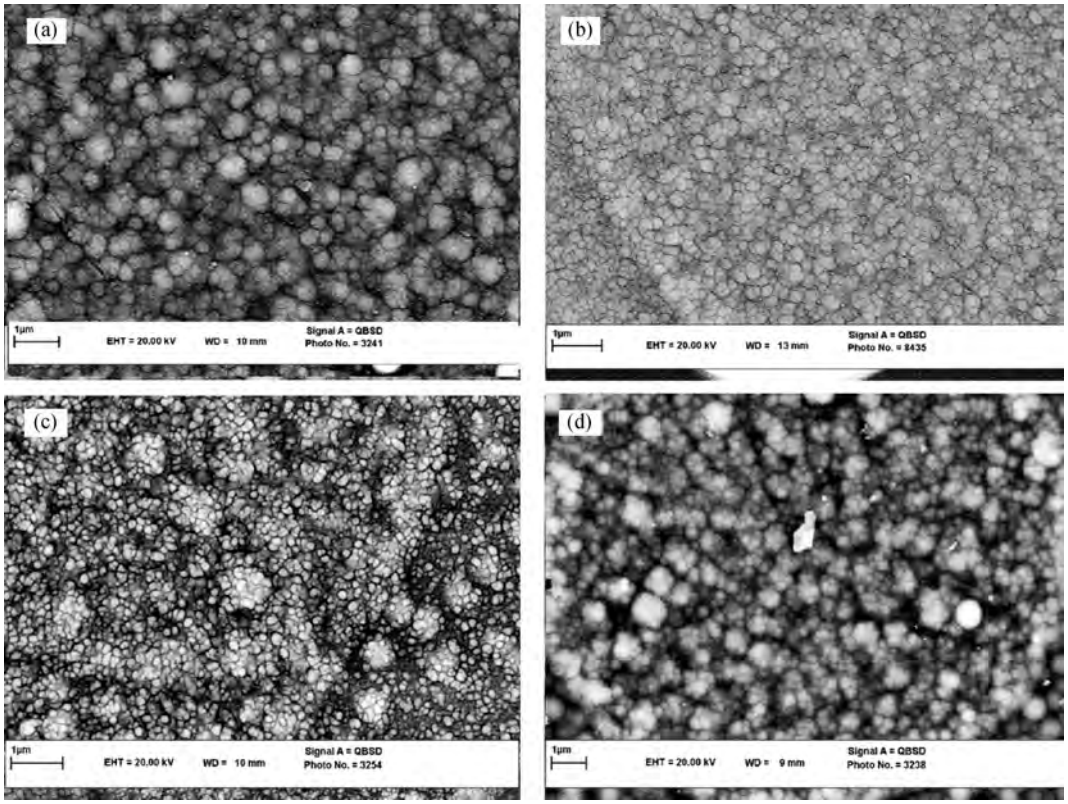

Fig. 6. SEM image of films prepared at (a) $T_s = 370$ ℃ and (b) $T_s = 420$ ℃ ($R = 10$ cc/min and $V = 100$ cc), (c) Rate = 15 mL/min ($T_s = 420$ ℃ and $V = 100$ cc) and (d) Volume = 150 cc ($T_s = 420$ ℃ and $R = 10$ cc/min).

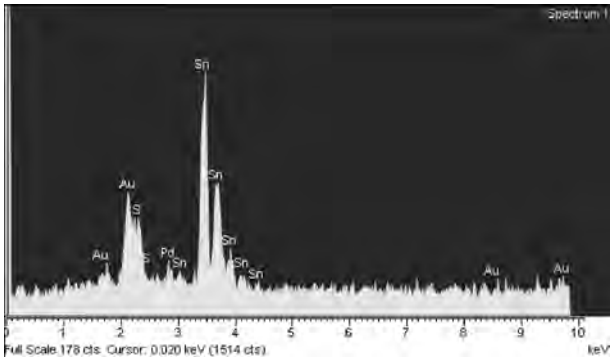

Fig. 7. EDX analysis for Sn_xS_y thin film prepared at Rate = 10 cc/min, $T_s = 420$ ℃ and $V = 100$ cc.

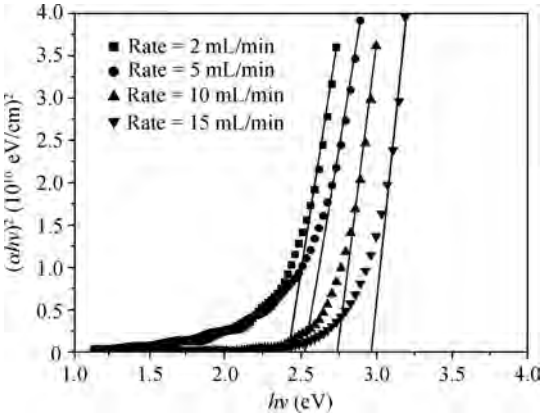

Fig. 8. $(\alpha h\nu)^2$ versus $h\nu$ of Sn_xS_y thin films prepared by various spray solution rates.

(b) $T_s = 420$ ℃ [$R = 10$ cc/min and $V = 100$ cc] , (c) Rate = 15 mL/min [$T_s = 420$ ℃ and $V = 100$ cc] and (d) Volume = 150 cc [$T_s = 420$ ℃ and $R = 10$ cc/min] have been shown in Fig. 6. We can see that with increasing the substrate temperature from 370 ℃ (Fig. 6(a)) to 420 ℃ (Fig. 6(b)), the size of grains becomes greater and the roughness of the surface is decreased. The poor crystallinity of the layers grown at low temperatures is probably due to the lack of thermal energy for the nucleation of deposited atoms and the formation of discrete islands in the films. We can also see that with increasing spray rate from 10 mL/min (Fig. 6(b)) to 15 mL/min (Fig. 6(c)) the tightly packed particles are decreased. We see that with increasing the solution volume from 100 (Fig. 6(b)) to 150 cc (Fig. 6(d)), the tightly packed particles decrease and the size of grains also increases. The averages of grain size using SEM images (Figs. 6(a)–6(d)) are ∼130, ∼200, ∼110 and 220 nm, respectively. However, the average grain size by SEM is larger than that we have calculated from Scherrer's formula by XRD patterns. Clearly, each particle in the SEM image contains many polycrystalline grains.

Figure 7 shows the EDX spectrum of the thin film prepared at Rate = 10 cc/min, $T_s = 420$ ℃ and $V = 100$ cc. Only Sn and S peaks are observed (expect Au as conducting coating), to confirm presence of S and Sn in thin films.

3.2. Optical properties

The optical band gap of the films in various deposition conditions is determined from the plot of $(\alpha h\nu)^2$ versus $h\nu$ as

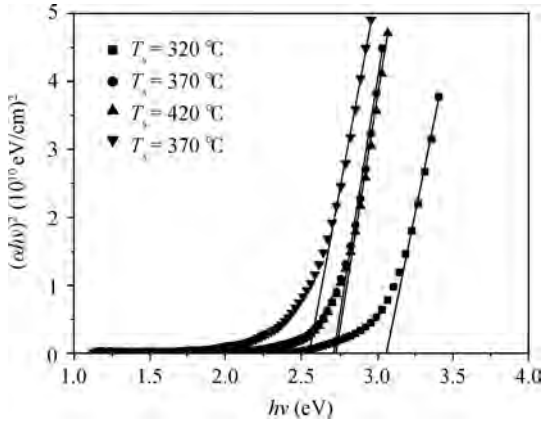

Fig. 9. $(\alpha h\nu)^2$ versus hν of Sn_xS_y thin films prepared by various substrate temperatures.

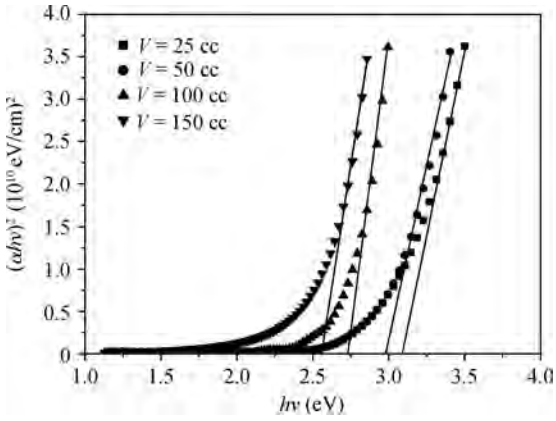

Fig. 10. $(\alpha h\nu)^2$ versus hν of Sn_xS_y thin films prepared by various spray solution volumes.

shown in Figs. 8–10. As can be seen, the plots are linear and indicate a direct optical transition. The results of the optical characterizations and electrical properties of the thin films have been summarized in Tables 3–5. These results indicate that with increasing the spray rate, the optical band gap of films is increased. Also, increasing the substrate temperature and volume of spray solution leads to an increase in the film thickness and grain size, as revealed by SEM images, and therefore decreasing the optical band gap of films.

3.3. Photoconductivity and thermo-electrical properties

The results of the photoconductivity and thermo-electrical measurements for Sn_xS_y thin films have been summarized in Tables 3–5. The measurement results of the dark electrical resistivity of the films show that with increasing the substrate temperature and volume of spray solution, the electrical resistivity is decreased due to (i) increasing the films thickness, (ii) high surface uniformity (as revealed by SEM images), and (iii) modification of structural order[13]. The high electrical resistivity of the prepared films at T_s < 370 ℃ is probably due to the presence of a SnS unstable compound or the formation of an amorphous phase. In addition, the smaller grainy structure or nearly amorphous structure may also contribute to the higher resistivity of the grown layers[8]. Decreasing the electrical resistivity in the dark with increasing the substrate temperature may be due to the increase in the crystallite size of the films[8, 15]. With increasing deposition temperature, the films become more polycrystalline and so the grain size of the films is improved[4]. The observed low resistivity of films at T_s = 470 ℃, is correlated to the presence of the Sn–O–S and SnO_2 semiconducting phases[8]. The decreasing dark electrical resistivity from 36.2 to1.66 Ω·cm with increasing the spray solution volume could be due to the increase in the film thickness.

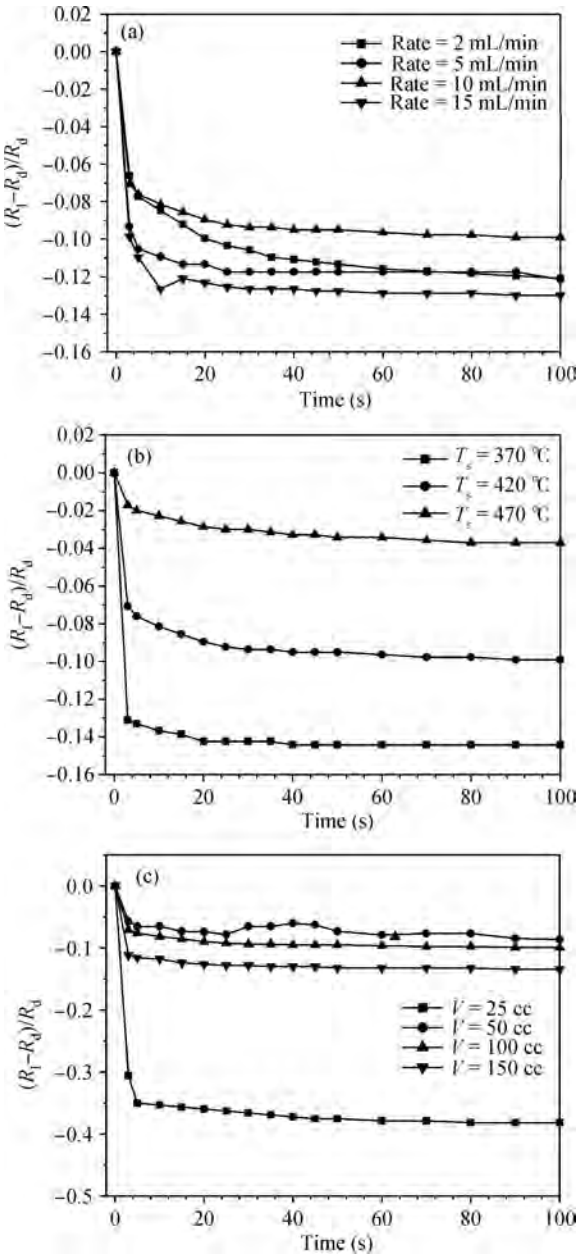

Fig. 11. (a) Variations of $\Delta R/R_d$ versus time of Sn_xS_y thin films prepared at various solution spray rates. (b) Variations of $\Delta R/R_d$ versus lighting time of Sn_xS_y thin films prepared at various substrate temperatures. (c) Variations of $\Delta R/R_d$ versus lighting time of Sn_xS_y thin films prepared with various spray solution volumes.

The photo-sensitivity (S) property of Sn_xS_y films is extremely related to substrate temperature and spray solution volume as shown in Tables 2, 3 and Figs. 11 (a)–11(c). It is increased by increasing the substrate temperature and spray so-

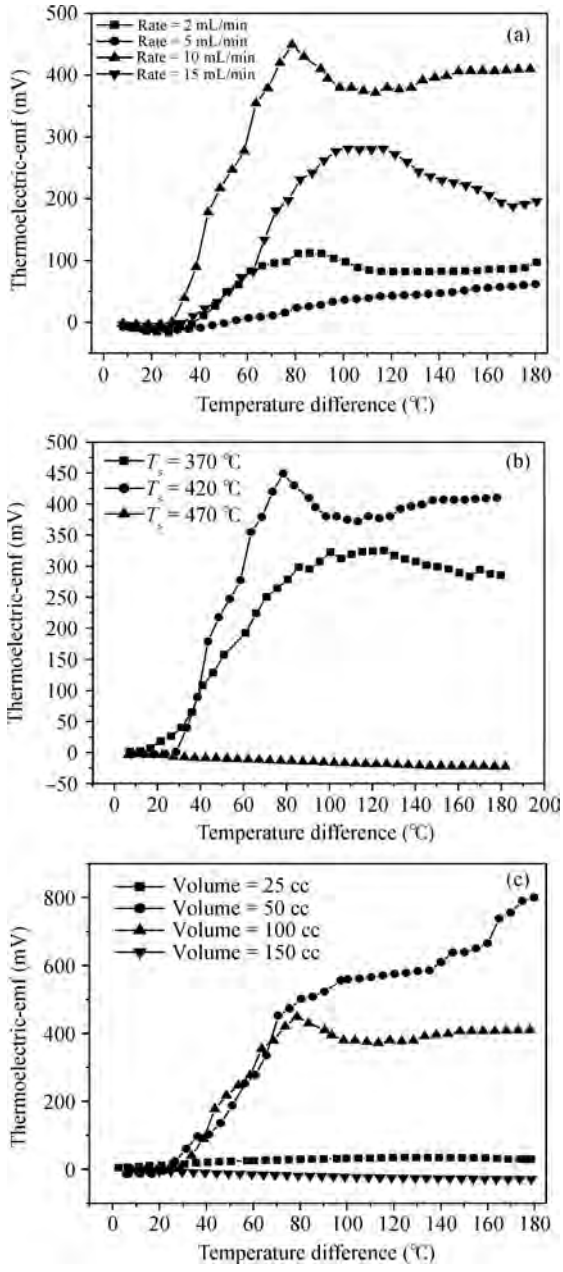

Fig. 12. Variation of thermoelectric e.m.f. with the temperature difference (δT) for Sn_xS_y thin films prepared by (a) various solution spray rates, (b) various substrate temperatures, and (c) various spray solution volumes.

lution volume due to decreasing the initial electrical resistivity. Indeed, we could change the photosensitivity of Sn_xS_y films by varying deposition conditions. The photosensitivity for all the films shows a behavior of exponential fall in resistance at first and then a tendency of saturation. The saturation condition is due to a decrease in the rate of photo-generation of carriers related to time. Simultaneously, the recombination process has a main role in reducing the photosensitivity. Consequently a steady state is obtained where the rate of generation of charge carriers is equal to the recombination rate under constant illumination. This phenomenon is responsible for obtaining a nearly flat profile of the photosensitivity at the end (see Fig. 11). A high photosensitivity of 0.4 was shown for prepared films at $T_s = 470$ ℃.

Figure 12 shows the variation of the thermoelectric e.m.f versus the temperature difference as a function of various deposition conditions. It shows that the absolute value of the thermoelectric e.m.f, $|\varepsilon|$, increases quickly with the increase in temperature difference at a low temperature difference range, which suggests the degenerate nature of thin films. The results of thermoelectric measurements indicate that prepared films with a spray solution volume of 150 cc and substrate temperature of 470 ℃ have n-type conductivity and the other films have p-type conductivity (see Tables 3–5). The prepared films with solution volumes of 100 and 50 cc have the best thermoelectric properties with $S = 4.6$ and 4.46 mV/K, respectively. The thermoelectric e.m.f depends on the location of the Fermi energy in the material and the type of scattering mechanism, and the charge carries encounter. It increases as the Fermi energy moves further into the energy gap from the bottom edge of the conduction band. This amounts to concluding that the smaller the carrier concentration, the larger the Seebeck coefficient. Thus, the relatively higher thermoelectric e.m.f for thin films is due to their higher crystallinity and crystallite size. The prepared films at a substrate temperature of 320 ℃ display a fluctuating nature in thermo-electrical e.m.f measurements, which may be due to the very high resistivity of films (See Figs. 12(a)–12(c)). The Sn_xS_y thin films show mostly p-type conductivity. The positive sign of thermoelectric e.m.f indicates that the conduction takes place due to the holes in the valence band, since the acceptor levels are created by the tin vacancies, they normally appear in the lattice[8, 16].

4. Conclusion

In this paper, to find the optimal parameters for the deposition of Sn_xS_y films three sets of experiments were carried out. The substrate temperature, volume and rate of spray solution were optimized for Sn_xS_y films that can be used as n or p-type light absorbed semiconductor thin film with a direct band gap suitable for solar cell applications. With control of suitable deposition conditions, we can prepare both n and p-type Sn_xS_y for fabrication of Sn_xS_y homo-junction and thermo-photovoltaic solar cells. Highly photosensitive Sn_xS_y films have wide potential applications as smart materials for saving energy.

References

[1] Cheng S Y, Chen G N, Chen Y Q, et al. Effect of deposition potential and bath temperature on the electrodeposition of SnS film. Opt Mater, 2006, 29: 439

[2] Deshpande N G, Sagade A A, Gudage Y G, et al. Growth and characterization of tin disulfide (SnS_2) thin film deposited by successive ionic layer adsorption and reaction (SILAR) technique. Journal of Alloys and Compounds, 2007, 436: 421

[3] Li Q, Ding Y, Wu H, et al. Fabrication of layered nanocrystallites SnS and β-SnS_2 Via a mild solution route. Materials Research Bulletin, 2002, 37: 925

[4] Reddy N K, Reddy K T R. Preparation and characterisation of sprayed tin sulphide films grown at different precursor concentrations. Mater Chem Phys, 2007, 102: 13

[5] Bagheri-Mohagheghi M M, Shokooh-Saremi M. Investigations on the physical properties of the SnO_2–ZnO transparent conduct-

ing binary–binary system deposited by spray pyrolysis technique. Thin Solid Films, 2003, 441: 238

[6] Bagheri-Mohagheghi M M, Shahtahmasebi N, Alinejad M R, et al. Fe-doped SnO_2 transparent semi-conducting thin films deposited by spray pyrolysis technique: Thermoelectric and p-type conductivity properties. Solid State Sci, 2009, 11: 233

[7] Sánchez-González J. Determination of optical properties in nanostructured thin filmsusing the Swanepoel method. Appl Surf Sci, 2006, 252: 6013

[8] Reddy N K, Reddy K T R. SnS films for photovoltaic applications: physical investigations on sprayed Sn_xS_y films. Physica B, 2005, 368: 25

[9] Bindu K, Nair P K. Semiconducting tin selenide thin films prepared by heating Se–Sn layers. Semicond Sci Technol, 2004, 19: 1384

[10] Nolas G S, Sharp J, Goldsmid H J. Thermoelectrics e basic principles and new materials developments. Berlin: Springer, 2001

[11] Li L, Fang L, Chen X M, et al. Influence of oxygen argon ratio on the structural, electrical, optical and thermoelectrical properties of Al-doped ZnO thin films. Physica E, 2008, 41: 169

[12] Calixto-Rodriguez M, Martinez H, Sanchez-Juarez A, et al. Structural, optical, and electrical properties of tin sulfide thin films grown by spray pyrolysis. Thin Solid Films, 2009, 517: 2497

[13] Devika M, Reddy N K, Ramesh K, et al. Influence of substrate temperature on surface structure and electrical resistivity of the evaporated tin sulphide films. Appl Surf Sci, 2006, 253: 1673

[14] Akkaria A, Guaschb C, Kamoun-Turkia N. Chemically deposited tin sulphide. Journal of Alloys and Compounds, 2010, 490: 180

[15] Reddy K T R, Reddy P P, Miles R W, et al. Investigations on SnS films deposited by spray pyrolysis. Opt Mater, 2001, 17: 295

[16] Thangaraju B, Kaliannan P. Spray pyrolytic deposition and characterization of SnS and SnS_2 thin films. J Phys D: Appl Phys, 2000, 33: 1054